Bird-inspired Velocity Optimization for Unmanned Aerial Vehicles in the Urban Environment

C.J. Williamson*, A. Spelt† and S. P. Windsor‡
Aerospace Department, University of Bristol, BS8 1TR, UK.

Small Unmanned Aerial Vehicles, SUAVs, are low-cost quick to launch platforms which offer potential for a range of roles in urban environments. However, these environments create complex wind flows that present control issues for small, low speed platforms. Further to this, battery technology does not yet offer the power-weight capacity to enable the endurance requirements for such missions. In comparison, birds of comparable size and weight are not only able to manage complex wind flow, but also exploit the environment as a locomotive energy source. Birds in migration are known to adjust airspeed to minimize the energetic cost of transport in response to wind conditions however, it is unknown whether birds implement the same velocity optimization strategies in more complex environments and while performing energy harvesting flight strategies. This study used Global Positioning System (GPS) backpacks to track 11 urban nesting gulls and found that during 193 daily commutes the gulls were able to soar 44% of the time by making use of both thermal and orographic updrafts. We outline cost of transport (CoT) theory and propose a model for optimizing airspeed for given wind conditions whilst maintaining a trajectory to a given location. We used the gull flight paths to test for CoT velocity adjustments by considering their flapping and soaring strategies. We found that by having a similar best glide speed and minimum power speed in soaring and flapping flight the gulls were able to make energy savings of as much as 30%. These models calculated optimum ground and airspeeds for known wind conditions assuming trajectory holding throughout flight, and as such could be implemented on a SUAV platform with wind sensing capabilities. This approach could significantly reduce the energy requirements for a SUAV navigating in an urban environment.

I. Nomenclature

$\beta_{a,i}$	=	angle between velocity and wind vectors in the air or inertial frame
D	=	aerodynamic drag force
E	=	energetic cost
e	=	error tracking
g	=	gravitational constant
$h_{AGL,HAS}$	=	altitude above ground level, height above structure
$k_{f,s}$	=	drag factor in flapping or soaring flight
m	=	body mass
ϕ_i	=	heading in the inertial frame
r	=	flight range
$S_{b,w}$	=	surface areas of body or wing
U	=	velocity in the air frame
$U_{bg,mp,mr,ms}$	=	best glide, minimum power, maximum range, minimum sink velocities
V	=	velocity in the inertial frame
V_z	=	sink speed in the inertial frame
W	=	wind speed
W_D	=	wind direction
$W_{a_{h,s}}$	=	head- or side-wind component in the air frame
$W_{i_{h,c}}$	=	head- or cross-wind component in the inertial frame
W_z	=	vertical wind component

*Research Associate, Aerospace Dept., University of Bristol, CAME School, Queen's Building, University Walk, BS8 1TR, UK.
†PhD Candidate, Aerospace Dept., University of Bristol, CAME School, Queen's Building, University Walk, BS8 1TR, UK.
‡Senior Lecturer, Aerospace Dept., University of Bristol, CAME School, Queen's Building, University Walk, BS8 1TR, UK.

II. Introduction

SMALL Unmanned Air Vehicles, SUAVs, have the potential to fly at low altitudes within the urban environment making them suitable for a range of missions such as infrastructure monitoring, surveillance, emergency response and small payload delivery [1–5]. However, current SUAVs have two main technology limitations, firstly, SUAVs have limited capacity to cope with the high levels of turbulence and complex flows created by wind interactions within the urban landscape [6–8]. Secondly, due to the power-weight constraints in battery technology, SUAVs have a limited range and endurance [9, 10]. This research takes a novel approach to finding ways of overcoming these limitations by looking at the ways birds make use of wind flows in the urban environment to reduce their energetic cost of flight.

Birds of comparable size and weight to small SUAVs are able to navigate the complex city wind flows and exploit the environment to reduce the energetic cost of flight. During the breeding season, urban gulls spend up to 40% [11] of their time in flight, flying to and from foraging locations through these complex wind-scapes. Choosing appropriate flight strategies has the potential to substantially reduce their energetic flight costs and could be key for breeding success. Understanding the energy saving strategies urban gulls are using to reduce flight costs could be used to extend the range and endurance of SUAVs flying in a similar environment.

The theory of flight mechanics describes the minimization of transport costs by adjusting airspeed with relation to the wind conditions. In unfavourable conditions such as headwinds, airspeed should be increased and in favourable conditions such as tailwinds, airspeed should be reduced. Vertical wind components also effect the transport costs, a down draft will increase the cost of transport and therefore airspeed should be increased, and an up draft will reduce the cost of transport, CoT, and so airspeed should be decreased. Gull species studied in migration and in long-range open water commutes were found to make velocity and even altitude adjustments to headwinds that act to maximize CoT savings [12, 13]. However, these flights tend to experience uniform and predictable flow conditions which are not representative of the urban environment.

A recent study found that urban gulls spend up to 10% more time in flight than those in traditional habitats [11], so it may be that the complex flows generated by our architecture creates more soaring opportunities than are available in more traditional habitats. Certainly studying gulls in this environment can provide new insight into managing these complex flows. Previous work found that gulls exploit the wind-highways generated by urban terrain [14] and a SUAV flight control strategy based on the gulls flight behaviour achieved a throttle reduction of 15% whilst minimizing overall control-effort [15]. Additional SUAV studies have found that exploiting urban flow can successfully be used to gain significant altitudes [16] and that choosing the correct airspeed and climb angles for the wind gradient can be used to make savings of 12% in the field [10]. Certainly then, studying birds in urban environments can present strategies which are advantageous to SUAV technology. However, there has been little research in the way free flying birds use wind flows in the urban environment, and whether velocity adaptions for CoT are universal to all flow fields.

This study aims to discern whether CoT velocity adaptions are advantageous when implemented in the complex flow conditions created by urban infrastructure using commuting urban gulls as a case study. Firstly, we outline relevant flight mechanics theories regarding velocity optimization before detailing a velocity optimization algorithm suitable for use when flying on a fixed heading with knowledge of current wind conditions. Following this, the methods used for capturing and analysing flight data from GPS tagged gulls is described, including how the data was down-selected and categorized into different soaring strategies. The velocity optimization models are then tested against the different flight strategies employed by the gulls to determine their potential for energy savings in urban environments.

III. Flight Models

This section contains the flight mechanics theory behind the velocity optimization models used throughout. The glide polar and mechanical power curve models used for the gulls are outlined along with the key velocities involved with optimizing flight performance. Following, is an explanation of CoT theory where the relationship between airspeed and the wind conditions is introduced. This relationship is used to outline an algorithm for calculating the optimum airspeed for a fixed trajectory and known wind conditions. Three potential flight speed selection models for flapping flight are then introduced.

A. Velocity curves

Avian flight has typically been studied at two very different scales. At one end of the spectrum, the precise mechanics and aerodynamics of flight has been studied in controlled environments such as wind tunnels, which has given rise to

detailed models used to predict flapping power requirements [17–19] and optimum glide ratios [20–23]. While on the broad scale, flight mechanics models have been used to study the energy saving techniques implemented by migratory birds in relation to weather systems [12, 13, 24–26].

Probably the most widely used glide polar model for birds was developed by Pennycuick and popularized by the Flight software [27]. This method calculates glider polars using the same methods as for fixed-wing aircraft, separating the induced aerodynamic drag force from the viscous drag generated by the friction over the wings and body. A power curve approach is then used to model flapping flight, with the induced drag being considered proportional to the absolute minimum power required to stay in flight, calculated by modelling the moving wings as an actuated disc [27].

The drag forces in flight vary with velocity in a manner which results in a minima in both the glide polar and the power curve, see figure 1. The airspeed at this minimum value represents the lowest energy exchange such that in flapping flight this is the velocity which requires minimum power and in gliding flight will result in the minimum sink rate, these will be referred to as the minimum power, U_{mp}, and minimum sink, U_{ms}, velocities respectively. Flying at these airspeeds will result in maximum flight endurance but does result in the lowest energy cost for a given distance. The lowest energy cost for transport can be found at the tangential to each of the curves, labelled in part e) of figure 1 and referred to as maximum range velocity, U_{mr} for flapping flight, and best glide velocity, U_{bg}, for gliding flight. These velocities are summarized in Table 1.

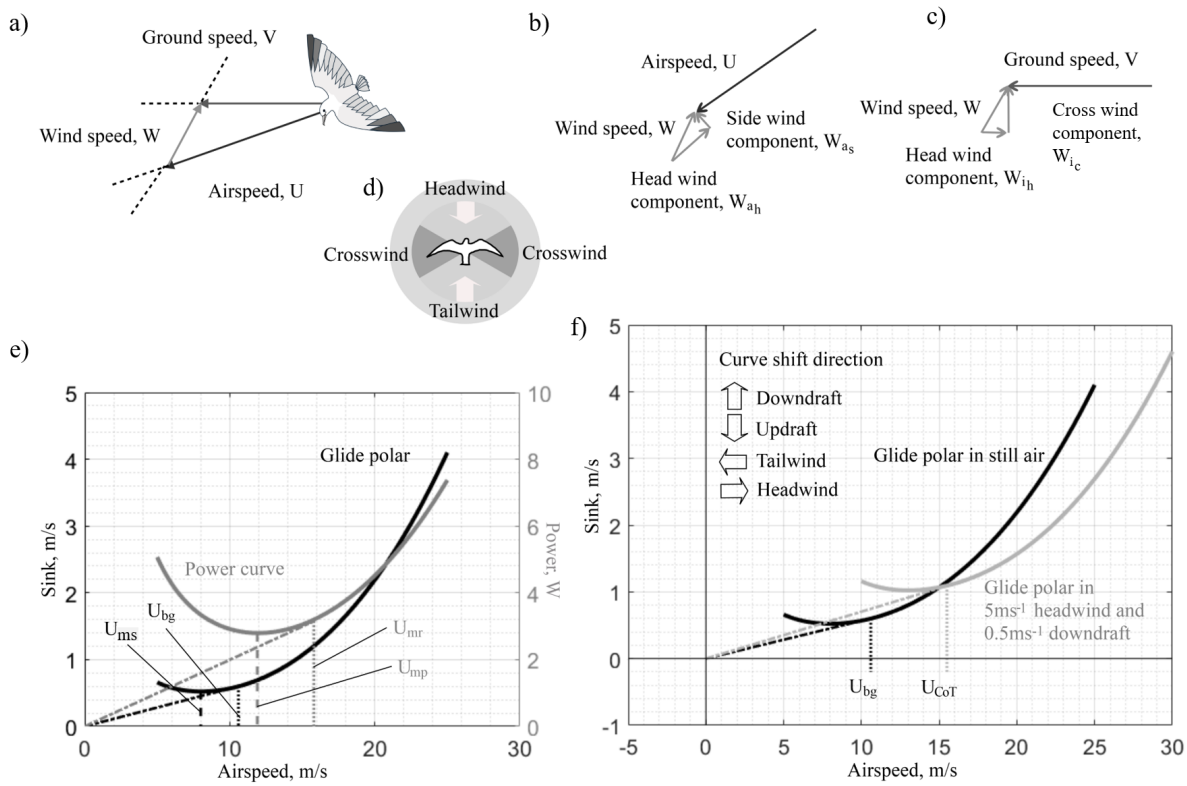

Fig. 1 a) Vector diagram of inertial, air and wind speed vectors. b-c) The head- and side-winds in the air and ground frames respectively. d) Definition of head-, cross-, and tail-wind angles where headwind is considered $\pm(0^\circ - 60^\circ)$, crosswind is $\pm(60^\circ - 120^\circ)$, and a tailwind is $\pm(120^\circ - 180^\circ)$. e) Glide polar and power curve for the average gull (Table 2). f) Curve shifting for head/tailwinds and up/downdrafts where the glide polar in still air is indicated by the black line and shifted curve is shown in gray.

The glide polar and power curve models were generated using equations and aerodynamic characteristics from Pennycuick's 2008 model [27] and collected gull bio-metrics (Table 2).

Table 1 Performance airspeeds for flapping and gliding flight for average gull

Velocity Name	Symbol	Airspeed, (ms^{-1})	Optimization
Flapping			
Minimum Power	U_{mp}	11.9	Endurance
Maximum Range	U_{mr}	15.4	Range
Gliding			
Minimum Sink	U_{ms}	8.2	Endurance
Best Glide	U_{mp}	10.6	Range

B. Cost of Transport Theory

When flying through a moving medium it is important to consider the effect of the substrate on relative motion. In CoT theory, overall energy cost is considered for the distance travelled but the direction and velocity of flow can effect progress in the world frame. The velocity reference frames can be seen in figure 1 and are considered in equation 1 where V is the ground speed, U is the airspeed and W is the wind speed.

$$U = V - W \tag{1}$$

Many studies have derived the necessary velocity changes required in order to maintain optimal flight cost [27–30]. In a recent study, Taylor et al, derived equation 2 which considered the cost of transport in the air reference frame, see part b) of figure 1. The energy cost, E, for a given range, r, is considered in terms of the thrust requirements, DU, for a given airspeed, U, minus the effect of any weight supporting vertical wind. The wind conditions, where W_h and W_s are the head- and side-wind components, also have an effect. In summary the equation shows that CoT is reduced by updrafts ($W_z > 0$) or tailwinds ($W_h < 0$) and increased in downdrafts ($W_z < 0$) or headwinds ($W_h > 0$).

$$-\frac{\mathrm{d}E}{\mathrm{d}r} = \frac{DU - mgW_z}{\sqrt{(U - W_{a_h})^2 + W_{a_s}}} \tag{2}$$

It should be noted that wind vectors, composed of head and side winds, can be considered in two ways aligning with reference to the air frame or the inertial frame, parts b) and c) in Figure 1 respectively. CoT is performed for a given distance so could be considered in the inertial frame [31], however in environmental harvesting strategies it is the airspeed in relation to the wind which should be optimized [30]. This study considers the wind vectors in the air and ground frame as side and cross winds respectively.

In gliding flight if the updraft is greater than the minimum sink rate the CoT optimization can break down as flying at a faster speed can still decrease the CoT. In this case it is possible to fly at speed which matches the sink rate on the glide polar. For glider pilots, the theory is best known as Speed to Fly (StF), or MacCready's theory, and was developed by MacCready in [28]. Calculating the new optimum airspeed in both StF and CoT can be achieved by shifting the glide polar for the experienced conditions as is depicted Figure 1 f. An updraft shifts the curve toward the x-axis, in CoT theory the optimized velocity tends to the minimum sink velocity until the updraft is equal to the minimum sink. In StF theory, the thermal strength can be much greater than the minimum sink value, here the optimized velocity increases again with the thermal strength.

Gulls soaring using orographic lift were found to position themselves such that sink was offset and altitude maintained rather than to benefit from increasing velocity [14], suggesting that they follow CoT during orographic soaring. However, several soaring species of bird have been found to follow MacCready's StF in inter-thermal glide sections so this will also be tested [32–34].

C. Velocity optimization algorithm

This section details a velocity optimization algorithm that can be used to generate the optimum airspeed for CoT minimization when flying on a fixed heading with knowledge of current wind conditions. An iterative process was used to calculate the optimum airspeed and resultant ground speed, this considered that as the airspeed changed the relative wind direction will also change as the gull adjusts air relative heading to compensate for slip and maintain inertial heading.

The trajectory holding assumption follows that daily commuting flight, lasting between 10-30 mins, are long enough for the bird to want to reduce energy costs, but short enough that using wind drift will not provide any total benefit.

Additionally, many of these commutes exhibit orographic soaring behavior in which following a ridge feature is vital to continue energy harvesting. This is also applicable for SUAV technology where holding a fixed trajectory is part of the mission plan.

1) Start with the non-adjusted optimum velocity (U_{bg} for gliding flight) being held as the airspeed. Calculate the angle between the wind and ground speed vector, β_i given the trajectory heading, h, wind speed, W, and direction, W_D.
$$\beta_i = \arcsin\left(W/U_{bg}\right)\sin\left(W_D - h\right) \tag{3}$$
2) Calculate the air relative wind direction, β_a.
$$\beta_a = 180 - ((W_D - h) + \beta_i) \tag{4}$$
3) Calculate the air relative headwind, W_{h_a}.
$$W_{h_a} = W\cos\beta_a \tag{5}$$
4) Shift the glide polar or power curve, as shown in figure 1, by the headwind component calculated in the previous step, and any vertical wind component. Resulting in a new airspeed, U_{opt}. This step can also be achieved using a look-up table as described in [30].
5) Calculate the new resultant ground speed, V using the assumption that the gulls are trajectory holding and that there is no slip.
$$V = \sqrt{(U_{opt}^2 + W^2 - 2U_{opt}W\cos\beta_a)} \tag{6}$$
6) Repeat with new air and ground speeds (holding trajectory heading, wind speed and wind direction constant), until the error, e, between the start and end air-speeds calculated for the loop is less than 0.1 ms^{-1}.
$$e = (U_{opt} - U) \tag{7}$$

D. Velocity test models

The velocity optimization models use the glide polar and power curves generated by the aerodynamic characteristics from Pennycuick's 2008 model [27] and the gulls bio-metrics in table 2. A fixed-wing variation to the glide polar model was used due to the sufficient similarity at airspeed of $16ms^{-1}$ and below (accounting for 69% of the data) to other methods which include span reduction. Optimized velocity was calculated by shifting the glide polar by the airspeed and/or vertical wind, and a new tangent calculated as described in part e) of figure 1. The power curve model for flapping flight was also generated using sampled gull bio-metrics and values from Pennycuick's 2008 Flight model with a drag factor, k, of 1.1 being used. Pennycuick predicts that gulls fly at minimum power velocity due to power constraints in the pectoral muscles [27] however, some literature suggests that this would mean no airspeed optimizations are required [13]. To test these theories we selected three models:

- Model 1 - Flying at minimum power speed but maintaining flight time. This model used U_{mp} as the optimum velocity but shifts airspeed only if there is a headwind. There is no adjustment from U_{mp} in tailwinds. The adjusted velocity is the minimum of the shifted curve.
- Model 2 - Flying at minimum power speed with no attempt at airspeed optimization, the only change being the effect of wind on the ground speed.
- Model 3 - Matching flight speed to fit a CoT optimized best glide velocity, U_{bg}. This models uses gliding flight optimization with the assumption that gulls are able to fly at a range of airspeeds for a relatively low change in power requirement and optimize as expected to exploit environmental energy in soar modes.

IV. Methods

This section includes details for the empirical data capture and processing. The gull tracking, details of environmental data sets, flight path filtering and the classification of soaring strategies are presented here.

A. Bird tagging

This research analysed the flight paths of 11 lesser black-backed gulls, *Larus fuscus*, tracked using GPS backpacks [35] over two breeding seasons in the city of Bristol, UK. All work was approved by the University of Bristol Animal Welfare and Ethical Review Body (UIN: UB /15/069). Bird handling and tagging was conducted under BTO permit A /2831, additional details can be found in [11]. Bio-metrics for the individuals were recorded at the time of capture used to characterize the morphology based aerodynamics of an average individual, as found in table 2.

Table 2 Wing and body measurements calculated from measured bio-metrics

	Span (m)	**Mass (kg)**	**Wing area (m^2)**	**Aspect ratio**	**Chord (m)**	**Frontal area (m^2)**
Mean, μ	1.15	0.741	0.168	7.85	0.146	0.0067
Standard Deviation, σ	0.065	0.061	0.018	0.63	0.011	0.00036

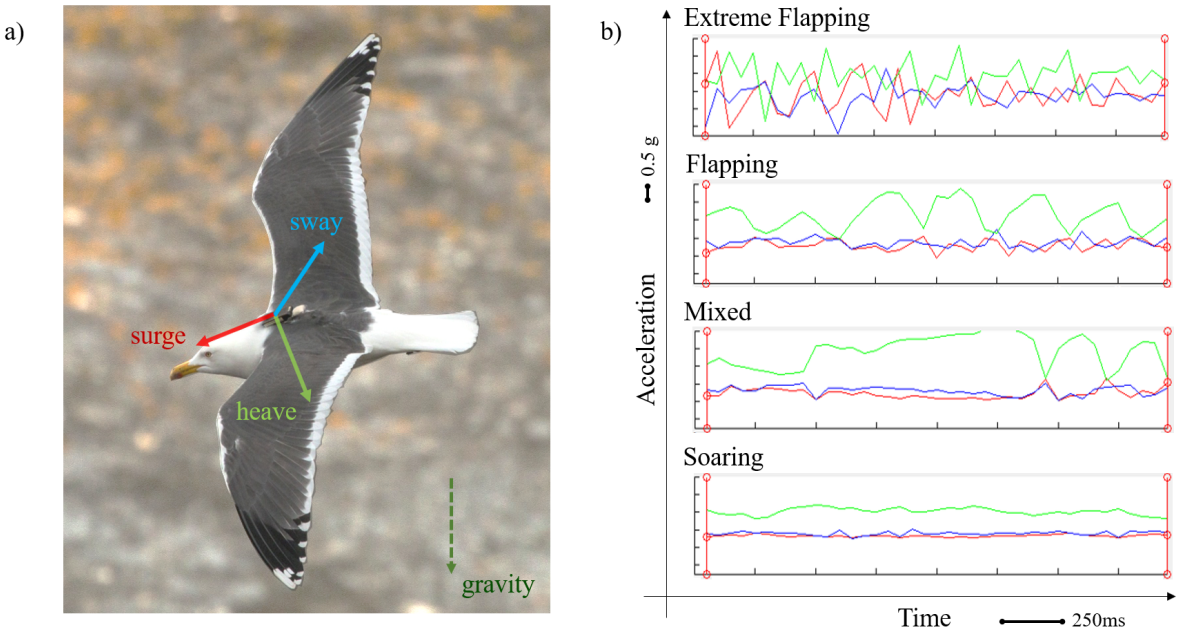

Fig. 2 a) Lesser black-backed gull with fitted GPS tag. b) The tri-axial accelerometer signals for four flight behaviors; extreme flapping, flapping, mixed and soaring as described in [11, 36]

B. Bio-logging data

The Global Positioning System, GPS, loggers collected a spatial fix containing latitude, longitude, altitude and a date-time stamp, each fix was immediately followed by a one second burst of 20 Hz three-axis accelerometer data. The spatial data were used to reconstruct the flight paths of the gulls and the acceleration data were used to characterize flight mode at each position. Details of the behavior classification can be found in [11, 36]. This study used four of these behavior classes; extreme flapping (such as in take-off and landing), flapping, soaring, mixed (combination of soaring and flapping), see Figure 2.

A spatial fence trigger was used to adjust the GPS capture frequency of the tags. When the gulls were on the nest, the capture rate was set to every a GPS fix every 10 mins (600 s). The devices were programmed to increase frequency to a minimum of every 5 mins (300 s) after leaving the nest, defined with a radius of 50 m. As a result outbound flights were often incomplete. The tags were charged by solar panels and when the tag had a sufficiently high battery voltage the tag switched to a high frequency data capture rate of every 4 s.

C. State variables

State variables associated with the flights such as velocity, altitude and attitude were calculated as follows. The ground speed of the gulls at the time of data capture was considered the instantaneous speed as calculated by satellite Doppler shift, as opposed to point-to-point differencing. Vertical and horizontal ground speeds were calculated separately in the case of gliding flight in order to compare forward and sink speeds. The altitude above sea level (ASL) was calculated using the GPS measured altitude. The altitude above ground level (AGL) and altitude above structure (HAS) were calculated using a digital elevation model from 2 meter resolution LIDAR data [37]. Heading and directional change angles were calculated using the latitude and longitude captured by the tags with a Haversine transformation adjusted for latitude at the nest location and accurate to 1%, which was considered accurate enough for the short point to point distances calculated.

D. Commuting Flights

Commuting flights were defined as non-stop flights between frequently visited locations. These flights were chosen under the assumption that the individuals are not foraging or searching, but travelling between known locations and as such, more likely to be conserving energy. The full data set was filtered to include only flights to and from 72 locations based on repeated visits. The locations were found using a combination of observation and spatial clustering of terrestrial location fixes. The commuting flight were defined using the filter criteria below:

- A series of flight behaviour data points enclosed by two terrestrial fixes at take-off and landing.
- A direct flight between the take-off and landing locations with no additional stops (terrestrial points).
- Start and end locations cannot be the same.
- A flight must have 10 or more fixes per km flown ensuring that trajectory resolution is suitably high.
- A flight must have more than 10 total fixes to ensure that flights are suitably long for evaluation.
- The flight must be repeated on 4 occasions such that there is a comparison set.
- Flights with obvious detours, foraging or loitering were removed.
- Start and end locations are at least 2 km apart.

This resulted in a set of 192 flights ranging between 2 and 20 km, with μ = 6.3 km, σ = 3.5 km.

E. Weather data

Weather data in this study was sampled from high resolution United Kingdom variable (UKV) forecasting model output data. The forecasting model has a spatial resolution of 2 km and a temporal resolution of 1 hour and has the highest resolution of any available data set over the UK [38]. Each GPS fix was assigned to the nearest 1-hour time prediction and then spatially interpolated. The wind speed and direction were interpolated for altitude and used to calculate airspeed. The forecast data were validated using data from a two week period collected by two locally situated weather stations; one at the nest and a second towards the North-East foraging areas. The Pearson produce-moment correlation coefficients computed for wind speed (R = 0.87, n >120,000, RMSE = 1.87ms^{-1}) and wind direction (R = 0.81, n>120,000, RMSE = 33.6°) showed that forecasting model gave wind estimates in good agreement with those measured directly.

F. Soar Strategies

Data points were given an additional flight mode classification based on the soaring strategies being utilized. All data points previously classified as soar behavior mode were further categorized into soar strategies; gliding (with subsets high and low altitude), thermalling, orographic and other using a decision tree classifier (Figure 3).

- Gliding is unpowered flight where gravitational and kinetic energies are traded. Here, it was defined as soaring behavior with a sink rate (downward vertical velocity) greater than 0.55ms^{-1}. This was selected as the minimum sink rate from the glide polar (Figure 1e). Classification of gliding was performed on the first branch of the decision tree (Figure 3). In some analysis gliding was further classified by altitude (AGL). High-altitude gliding such as between thermals, (Figure 4a), was classified by the same altitude threshold as the second branch in the decision tree. Low-altitude gliding was defined as below this threshold and occurred between sections of flapping, mixed or orographic soaring modes.

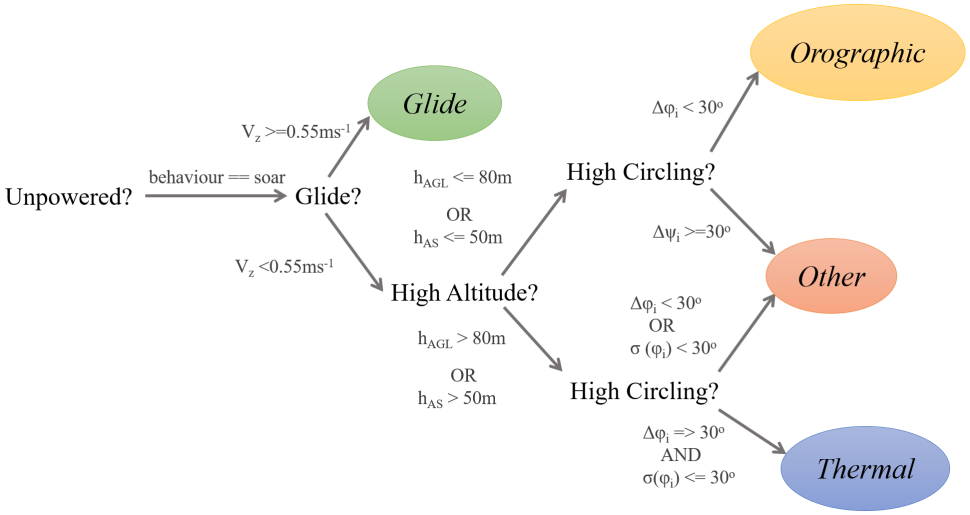

Fig. 3 Flight strategy decision tree with threshold values. The first branch sorts by flight behavior. The second branch sorts gliding or soaring. The third branch sorts using two altitude thresholds. The final branch sorts by heading change.

- In thermal soaring altitude is gained by circling in columns of warm rising air, as shown in Figure 4a. This was characterized firstly by high altitude flight where both altitude above ground level, h_{AGL} and height above surface structure, h_{HAS}, were considered. Secondly, by a high variance in flight direction, $\sigma(\phi_i)$, and a consistent heading change, $\Delta\phi_i$, of 30°or greater between fixes, shown by the final lower branch of the decision tree (Figure 3).
- Orographic soaring uses updrafts on the windward side of a terrain ridge feature, such as a cliff, hill or building, to offset sink in gliding flight. It requires a relatively low altitude to be within range of any updrafts. Examples of orographic soaring can be seen in Figure 4b,c. The strategy was classified when below the circling and altitude thresholds, as seen in the upper final branch of the decision tree (Figure 3).
- Other contains any soaring behavior which does not fall into the previous categories. This class contains a small fraction of low altitude thermalling or circling which could be a result of an area of very strong orographic lift, see examples Figure 4c, but mostly contains high-altitude soaring with no directional variance. This is most likely travel through unexploited thermals or detached thermal bubbles, an example of this is shown in Figure 4a.

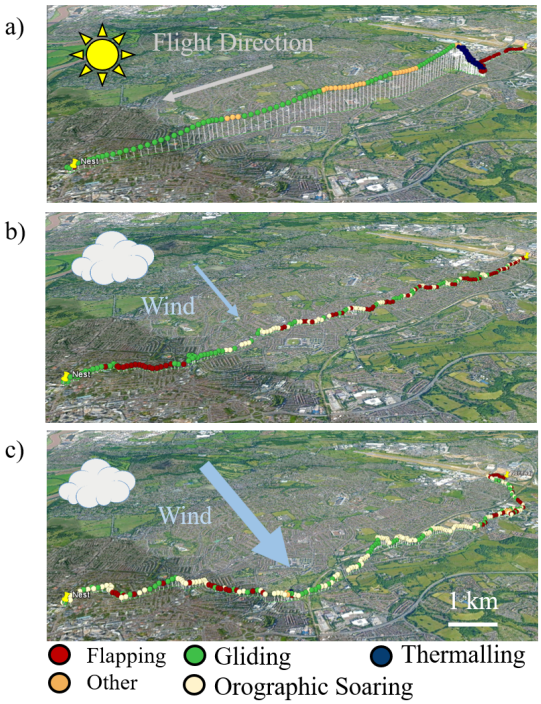

Fig. 4 Flights from the same individual that occurred with 3 different weather conditions. a) high thermal availability b) overcast day with low westerly wind c) day with a high westerly wind. Background courtesy of Google Earth [39].

Soaring strategy classification was validated with three methods. Firstly, by expert comparison with a set of 10 selected flights across the range of soaring strategies. Secondly, using a systematic variation of the threshold values to check for classification robustness. Thirdly by using a machine learning classification model trained with algorithm classified data and input variables from a geophysical, meteorological and time of day data set as found in [14]. Specifically, thermal and orographic flight strategies were tested as these strategies occurred in different conditions. The Classification Learner toolbox in MATLAB 2018a was used with a medium grain, k-clustering algorithm and a 5-fold test-train ratio. The classification of thermal and orographic points was found to agree with the decision tree algorithm with a 95% accuracy.

G. Inter-thermal gliding

Inter-thermal samples were generated by finding thermal-glide pairs that fall within three criteria; firstly, there must be 5 or more consecutive thermal points in the initial and subsequent thermals, secondly, the glide section joining the two thermal sections must contain more than 50% gliding strategy data with a low directional variance, and finally, all thermal-glide data must be high frequency data. All commuting flights were searched for thermal-glide pairs giving a total of 19 high-quality thermal-glide pairs. The thermal climb rate was calculated as the average vertical velocity and the inter-thermal velocity was calculated as the average airspeed performed over the entire glide sequence between thermals.

V. Results

A. Time budgets and soaring strategies

When flying in the urban environment the gulls were able to make extensive use of environmental energy, soaring 30% of the time (Figure 5b). This increased to 44% when just commuting flight was considered (Figure 5 c). The gulls used a mix of different gliding and soaring strategies, (Figure 5d), the most common combination being thermal soaring followed by sections of high-altitude gliding and occasional soaring (labelled other) through updraft pockets such as thermal bubbles. On days with low thermal availability but some wind, orographic soaring was also used extensively in combination with low-altitude gliding and mixed flight.

The percentage of thermal soaring suggests that the urban environment provides a significant level of thermal availability. Commuting flights that used thermalling were recorded with high percentages of non-flapping flight, with some flights containing as much as 100% soaring flight. These flights also contained soaring consistent with passing through thermals or thermal bubbles without circling to gain altitude and without the need to deviating significantly from the shortest commute path suggesting there is was a greater number of thermals available than required.

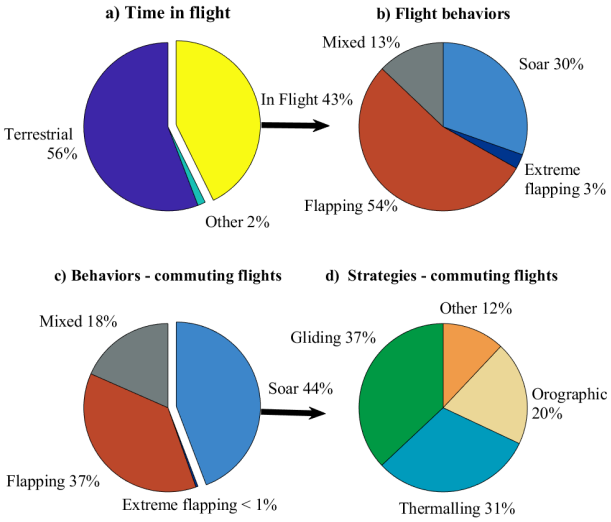

Fig. 5 a) Time budgets for terrestrial and in-flight behavior. b) Time budgets for in-flight behavior c) Commuting flight behaviors d) Soaring strategies used in commuting flights, with low- and high- altitude gliding being grouped.

The urban environment offered soaring opportunities when there was little or no thermal availability. These flights contained a mix of orographic soaring, low-altitude gliding and mixed flight and on average contained a higher fraction of flapping flight that thermalling flights. Flights featuring orographic soaring also featured higher levels of mixed behavior, with some flights featuring as much as 60% soaring flight and 40% mixed, and no flapping flight. It was expected that orographic updraft availability would be higher on days with stronger winds and as such these conditions would feature a higher percentage of orographic soaring. However, orographic soaring showed only a small increase with wind speed compared to a significant decrease in flapping flight and an increase in mixed flight. The percentage of orographic soaring increased with relation to the wind speed with a positive Pearson correlation ($R = 0.19, n = 2623, p < 0.001$), which could suggest the gulls were able to make use of orographic updrafts across a

range of wind speeds. The percentage of flapping was found to decrease with increasing wind speed with a negative correlation ($R = -0.34, n = 11285, p < 0.001$). The relatively low correlation could be explained by an absence of flapping flight on days with low wind speeds and high thermal availability. Mixed flight, however, was found to increase with wind speed with a strong positive correlation ($R = 0.64, n = 5829, p < 0.001$). Overall, these changes in behaviors in relation to wind speed indicates that the gulls were able to make use of the higher environmental energy available on windy days, but may have had higher control demands as represented by the higher level of mixed manoeuvring flight.

B. Airspeeds of flight behaviors and soar strategies

The gulls were found to have different airspeeds depending on their flight behavior or soaring strategy, (Table 3). In flapping and soaring flight, the gulls flew at velocities slightly below the predicted minimum power, U_{mp} = 11.9 ms^{-1}, and best glide, U_{bg} = 10.6 ms^{-1}, velocities respectively. The mixed flight average airspeed was considerably higher and could be associated with gusts and fast corrective manoeuvres. Unexpectedly, the average velocity in soaring flight was slightly higher than that in flapping flight, however the difference was not significant.

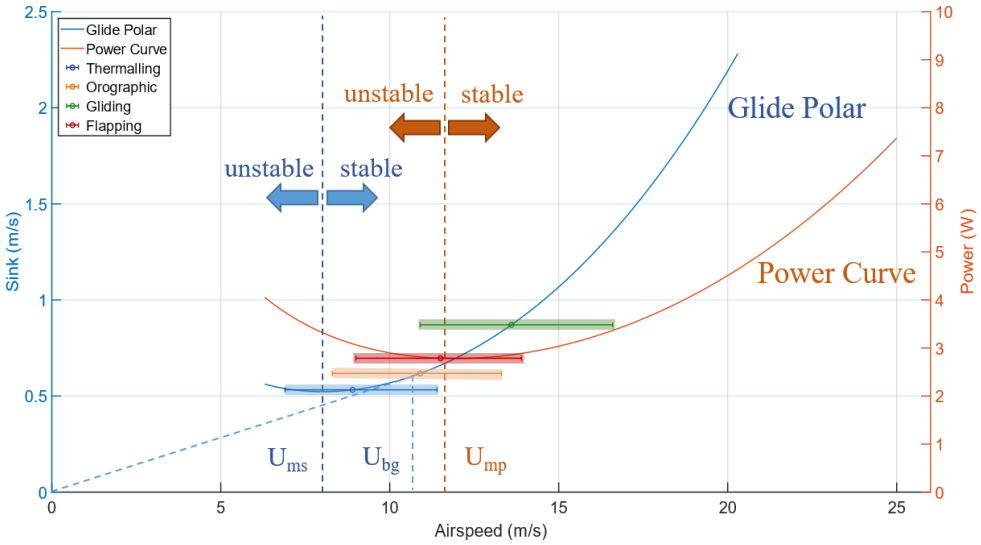

Fig. 6 Glide polar (blue) and power curve (orange) shown with the airspeeds for soar strategies thermal (blue), orographic (yellow) and inter-thermal (green), and flapping flight (red). The mean airspeeds are indicated by a dot and the bar indicates the standard deviation. The stable and unstable regions of each curve are also indicated and labelled. Min power, min sink and best glide velocities are indicated by the dashed lines for reference.

The altitudes flown by the gulls varied from 0 to 923 m (AGL) where the median altitude flown on non thermalling days was 34 m. When thermalling the gulls thermalled to a mean maximum altitude of over 600 m. To make velocities comparable equivalent airspeeds are used, taking into account the increase in velocity at altitude due to lower air density. When soaring strategies were compared using an ANOVA, all the airspeed distributions were found to be statistically different from flapping flight and each other, apart from the low altitude gliding and other soaring strategies, which were significantly different from flapping flight but not from each other. Interestingly, the high altitude gliding, such as between thermals was faster than the low altitude gliding, such as between intermittent flapping or orographic soaring ($f_{high-low}$=619, p***).

Thermalling flight, indicated in Figure 6 in blue, had the lowest average velocity at 9.6 ms^{-1}, and was close to the minimum sink velocity at 8.2 ms^{-1}, which would provide the best altitude gain but was still fast enough to avoid stall. During orographic soaring the average airspeed was 10.9 ms^{-1}, close to the best glide velocity for soaring flight, at 10.6 ms^{-1}. The average gliding airspeed was much higher at 13.8 ms^{-1} and was significantly higher than the best glide velocity (p<0.001).

Table 3 Airspeeds for flight behaviors and soar strategies

Flight type	Mean μ (ms^{-1})	Standard deviation σ (ms^{-1})	ANOVA f-value	p-value
Flight behaviors				
Flap	11.4	3.7	$f_{flap-soar}$ = 0.95	p = 0.33
Soar	11.9	4.4	$f_{soar-mix}$ = 134,	p***
Mixed	12.7	4.6	$f_{flap-mix}$ = 176,	p***
Soar strategies				
Thermal	9.6	3.7	$f_{therm-flap}$ = 1870	p***
			$f_{therm-soar}$ = 1091	p***
Orographic	10.9	3.8	$f_{oro-flap}$ = 75	p***
			$f_{oro-soar}$ = 62	p***
Other	12.3	4.6	$f_{oth-flap}$ = 26	p***
			$f_{oth-soar}$ = 32	p***
Gliding (all)	13.8	4.5	$f_{glide-flap}$ = 20	p***
			$f_{glide-soar}$ = 26	p***
Gliding (low altitude)	11.7	3.2	$f_{low-flap}$ = 2493	p***
			$f_{low-soar}$ = 1786	p***
Gliding (high altitude)	14.8	4.7	$f_{high-flap}$ = 2074	p***
			$f_{high-soar}$ = 992	p***
Where p significance levels are p*<0.05, p<0.01, p***<0.001**				

C. Airspeed optimization in soaring strategies

The gulls used different airspeed adaptions in relation to the relative wind direction depending on the soaring strategy being used. The relationships between airspeed and the air relative wind direction are plotted for four soaring strategies (Figure 7), and demonstrate the different airspeed adaptions used in each strategy.

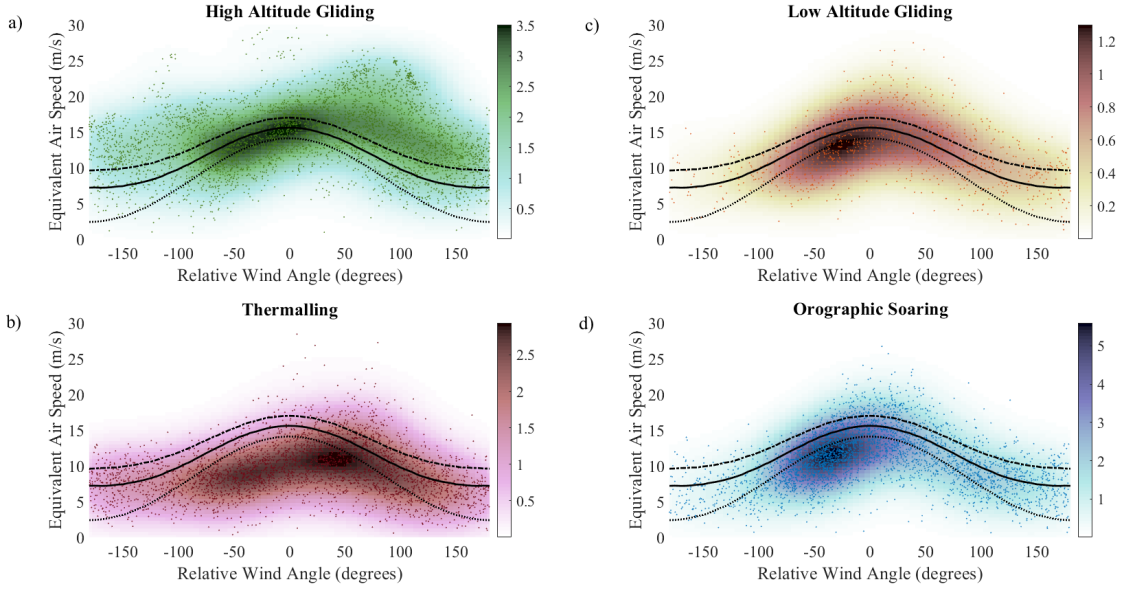

Fig. 7 Equivalent airspeeds at the relative wind direction compared to CoT model a) High altitude gliding flight b) Thermal soaring c) Low altitude gliding flight c) Orographic soaring. The central line in each plot is the optimum CoT airspeed for a 6 ms^{-1} wind with no updraft, the upper line is the optimum with an added downdraft of -0.5 ms^{-1}, and the lower line is the optimum for an added updraft of 0.5 ms^{-1}. The gull data shown is for airspeeds between 4.5 and 7.5 ms^{-1}. A Gaussian filter is used alongside the gull data to demonstrate density.

In high altitude gliding the gulls made the expected adjustments for the wind direction but flew slightly faster than expected (Figure 7a), as shown by the data following the shape of the curve but with many points higher than the predicted CoT optimum. In thermalling flight the gulls made relatively little adjustment to their airspeed for the relative wind direction (Figure 7b), as shown by their consistent airspeed for all relative wind directions. The gulls did make adjustments for the wind direction during low altitude gliding and orographic soaring (Figure 7c,d), where it can be seen that the gulls followed the predicted model except around a relative wind direction of 50°. This angle corresponds to a cross-wind in the inertial frame and would occur when flying along an object facing perpendicular to the wind. Here the gulls flew slower than predicted by the CoT model.

The airspeed data and model both use the measured wind conditions in their calculations which could introduce false correlation. In order to show that this did not effect the reliability of the model, ground speed predictions are also compared with the direct velocity measurements of the gulls (Appendix VIII.A) and showed that the results were consistent using either airspeed or groundspeed.

D. Inter-thermalling

During high-altitude gliding the gulls flew faster than the best glide velocity so it was expected that the gulls would fly at an airspeed described by MacCready's StF theory, shown as a dashed line in Figure 8. However, the results showed that the gulls flew slower than the optimum cross-country speed, as shown by the 19 inter-thermal flights indicated by the filled markers.

A second model using headwind adjustments and thermal strength is shown with square markers and also over predicts the flight speeds. Modelling the airspeed using CoT adjustments for horizontal wind is indicated by the vertical crosses and gave a much closer approximate to the measured gull airspeeds.

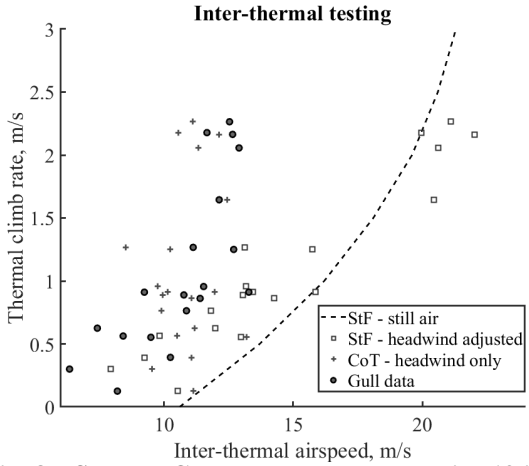

Fig. 8 StF and CoT models compared with 19 inter-thermalling flights.

E. Flapping flight and wind direction

During flapping flight the gulls appear to fly at their best glide speed modified for the relative wind direction according to CoT theory, as represented by Model 3 colored green in Figure 9. The mean ground speed predicted by adjusting best glide velocity for the head and cross winds conditions experienced by the gulls was a close match to the flight speeds recorded, while the model slightly under estimated the ground speeds flown by the gulls during a tailwind. Using a model which adjusted minimum power airspeed to maintain minimum flight duration (Model 1 shown in white) produced an over estimate of ground speeds for head and cross winds and also under estimated the ground speed in tailwinds. Meanwhile maintaining minimum power velocity regardless of the wind conditions (Model 2 shown in pink) produced a good estimate of ground speed in crosswinds but under-estimated in headwinds and over-estimated in tailwinds.

The gulls minimum power velocity is only slightly above their best glide velocity. This means that transitioning from soaring flight to flapping flight can be done efficiently without requiring a large power output for acceleration. This suggests that flapping at a velocity close to the best glide speed could be advantageous in complex flow environments

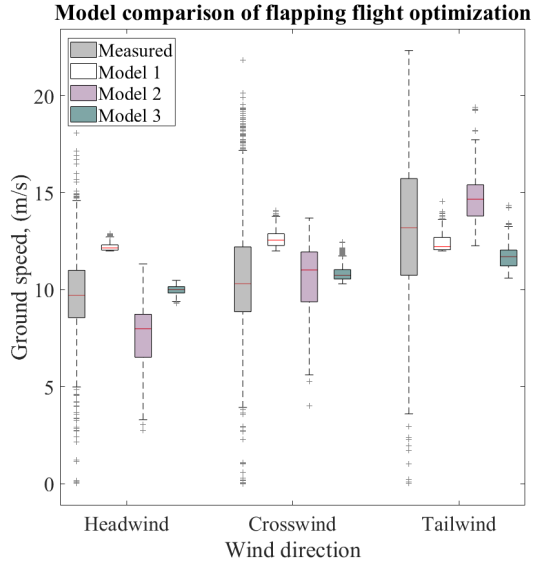

Fig. 9 Measured ground speeds taken from GPS compared against 3 models, model 1: Optimizing for U_{mp} and shifting with headwind, model 2: Maintaining U_{mp} regardless of headwind, model 3: Optimizing to match U_{bg} and shifting with headwind.

where updrafts are readily available. This could facilitate energy harvesting where the mechanical power requirements at the mean airspeed for head- and tail-winds, correspond to only a +6% rise from the minimum power requirement, as seen in Table 4. The average airspeeds, shown in Table 4 indicate that when orographic soaring the gulls slow down in cross and tailwinds, which both offer favourable CoT conditions. In gliding flight the gulls airspeeds are higher, indicating either an absence of updrafts or that the birds are not exploiting them.

Table 4 Mean airspeeds for wind conditions

	Wind Direction		
	Headwind	*Crosswind*	*Tailwind*
Flap			
Mean airspeed, μ (ms^{-1})	14.8	11.8	9.2
Power at mean airspeed, (W)	3.0, (+6%)	2.8, (U_{mp})	3.0, (+6%)
Standard deviation, σ (ms^{-1})	3.2	2.8	3.1
Sample size, n	3408	5417	2460
ANOVA f-values	$f_{head-cross}$ = 1184	$f_{cross-tail}$ = 1856	$f_{tail-head}$ = 4769
ANOVA p-values	p***	p***	p***
Orographic			
Mean airspeed, μ (ms^{-1})	14.2	11.0	7.4
Standard deviation σ (ms^{-1})	2.9	2.5	2.7
Sample size, n	916	1199	508
ANOVA f-values	$f_{head-cross}$ = 658	$f_{cross-tail}$ = 633	$f_{tail-head}$ = 1935
ANOVA p-values	p***	p***	p***
Gliding (low altitude)			
Mean airspeed, μ (ms^{-1})	15.3	12.5	9.6
Standard deviation σ (ms^{-1})	3.3	3.4	3.8
Sample size, n	584	1058	731
ANOVA f-values	$f_{head-cross}$ = 221	$f_{cross-tail}$ = 314	$f_{tail-head}$ = 901
ANOVA p-values	p***	p***	p***
Where p significance levels are p*<0.05, p<0.01, p***<0.001**			

VI. Discussion

With the increase in SUAV technology, the fine-scale flight strategies of birds offers inspiration for improved methods of energy harvesting. Implementation of avian soaring strategies on SUAV technology has the potential to greatly increase both endurance and range performance which would otherwise be restricted by the relatively low on-board power capacity. However, studies in this area are often performed via simulation [15, 40–43] or in comparatively simple flow conditions [10, 34]. This study considers that urban nesting gulls could offer valuable insight into the flight strategies suitable for the complex flow environment generated by city landscapes.

We tracked the flights of 11 urban nesting gulls using GPS loggers which allowed the measurement of their positional, velocity and behavior. The gulls were able to harvest environments energy extensively during their daily commutes using a combination of different soaring strategies by exploiting thermal and orographic updrafts. It is already known that urban building materials, such as concrete and asphalt, cause urban heat island effects [44, 45] so it follows that an abundance of these materials also generate the high levels of thermal updrafts that these gulls were seen to exploit. Additionally, gulls have been shown to use man-made infrastructures for orographic soaring in coastal areas where the buildings act as a synthetic cliff [14], this study indicates that this can be extrapolated over cities where the urban canyons create a network of wind-highways for soaring. Clearly, there is a large source of environmental energy within the urban environment available for harvesting in soaring flight. This suggests that SUAVs designed with soaring capabilities could be able to drastically reduce their flight costs during urban missions given the right control schemes.

A. Soaring strategies

The gulls used different strategies and airspeeds to harvest energy from different environmental sources. We found that the gulls made the greatest use of thermal updrafts combining this with high altitude gliding. In thermalling flight their airspeed remained close to their minimum sink velocity regardless of wind direction. Using a low airspeed promotes maximum altitude gains by requiring the lowest sink offset. In gliding flight, the minimum sink and stall speeds are extremely close; the minimum sink speed lies at the boundary of the unstable velocity region where a small decrease in velocity could result in deceleration to the stall speed [27, 46]. Flying within a small safety margin above the minimum sink alleviates risk which is particularly important when flying in crowded thermals [47]. Glider pilots and other bird species have also been found to make this same risk mitigating compromise [33, 34, 48].

When gliding between thermals, the gulls made use of CoT optimization for horizontal winds and although results indicate that there may be some velocity adjustment for updraft, the gulls did not fly at the high speeds predicted by StF. It is possible that the gulls did not perform StF due to an apparent abundance of thermal availability. The gulls were also seen performing straight soaring, non-gliding, flight between thermals consistent with flying through a thermal or thermal bubble [49] but not circling . Flying at a glide speed slightly above the best glide could mean the gulls are able to make use of the updrafts without overly extending the flight time. This could be particularly relevant during chick rearing period where time away from the nest could impact breeding success. Interestingly, a recent simulation study optimizing the velocity of UAVs in inter-thermal flight [50] found evidence which could support this theory. The study found that inter-thermal flight was optimal at a velocity between the best glide and StF velocities. The best glide velocity optimizes for the energy cost per distance whereas the MacCready predicted velocity provides the overall best flight time when considering the time required to gain altitude. For the gulls this suggests that while CoT is an important factor, that time away from the nest could also be an important driver.

The gulls were also able to perform high levels of soaring flight during periods of low thermal availability. In these cases, they performed a combination of flapping, gliding and orographic soaring flight. The orographic soaring analysis showed that the gulls flew slower than expected when making CoT adjustments for headwinds alone indicating that the gulls are making use of orographic updrafts available in the cities. Other bird species have also been found to reduce airspeed in orographic soaring when compared to straight gliding [32] further supporting the gulls' exploitation of orographic lift. Surprisingly, the orographic soaring was not limited to wind directions consistent with soaring in parallel to ridge features. Flying with a tailwind over terrain features provides updrafts on the windward side of the feature, followed by a section of downdraft on the leeward side. Gulls flying perpendicularly over buildings could use the updraft on the windward side gain altitude for clearance over the building. This could explain the large range of velocities measured in tailwinds and suggests gulls or SUAVs should slow down through the updraft on windward side of building and speed up through the leeward downdraft to harvest as much energy as possible.

B. Wing morphology

Wing morphology has a profound effect on the gulls' velocity envelope. Gulls have a relatively low wing loading like many soaring birds, but when compared to other marine bird species (such as albatross) they have a lower aspect ratio. The low wing loading results in being able to circle in narrow thermals but means a lower cross-country speed [32]. The gulls have a much lower wing loading (44N/m2) than that of the gliders (80+ N/m2) and some other thermalling bird species [32, 34]. Perhaps the gulls' low wing loading influences the cross-country speeds more than predicted in the StF model. We explored the wing loading constraints on velocity by comparing the flown airspeeds against a velocity envelope generated using FAR 23.333 regulations for light aircraft [51] and found that the maximum airspeed for a gull-sized platform would be 21 ms^{-1} (Appendix VIII.B), a speed that would be reserved only for extreme manoeuvre cases. While the low wing loading of the gull may limit their glide speed, their wing aspect ratio could have, in part, led to their success in urban environments. A relatively low aspect ratio results in greater wing-beat power which could be beneficial to the gulls three-fold. Firstly, by facilitating ground based take-offs. Secondly, by assisting in high-powered manoeuvres that could be required when navigating around obstacles. Finally, in the extreme flapping behaviour as seen during foraging [11]. However, the aspect ratio of the gull wing is in no doubt a trade-off, the gulls have a large enough aspect ratio to provide a relatively high glide ratio of 15 and a low minimum power cost in flapping flight.

C. Energy savings

The flight speeds of orographic soaring, low-altitude gliding and flapping flight are very similar, suggesting that matching the flapping speed to the soaring speed could have energy saving benefits. In flapping flight alone, the energetically cheapest speed to fly for a given distance is the maximum range velocity. Flying at maximum range

equates to a 14% saving compared to flying the same distance at minimum power velocity. Here when the average 44% soaring behavior is added to the calculation, there is a 35% energy reduction compared to flying at maximum range velocity, demonstrating an obvious potential benefit to flying at the minimum power velocity. Furthermore, the shallow minima of the power curve encompasses the velocity ranges required for all wind directions with only a +6% increase in mechanical power from the minimum power requirement, even with this power increase accounted for the energy savings would be 31%.

SUAVs could benefit from this speed matching strategy by taking into account the best performance velocities during the design phase of the platform. Matching the minimum power and best glide velocities for a platform would result in efficient use of environmental energy while demanding the lowest mechanical power for a motor when environmental energy sources are unavailable. Additionally, the performance curves of the platforms should have wide shallow minima to facilitate velocity matching for a wide range of wind speeds and result in low sink speeds. The FAR regulations for a gull sized platform resulted in relatively low maximum velocities however, as SUAV platforms do not require the same wing beat power demands as gulls, the aspect ratio can be increased, further reducing mechanical power demand.

Applying the optimized airspeed adjustments on SUAVs requires information regarding the heading trajectory and the wind conditions. Current on-board sensors record airspeed and trajectory heading, however the exact wind conditions are not measured. There have been recent developments regarding flow sensing in flight, where the wind conditions can be calculated using the differential airspeed sensors [52], distributed pressure sensors [53], and estimated by tracking the drift of the vehicle when circling [54]. As these techniques continue to improve, airspeed matching that facilitates energy harvesting may become more common place too. Current energy harvesting methods focus on locating updrafts, however platforms in the future, such those designed for smart cities [55, 56], may need to follow strict trajectories. The methods used by the gulls suggests that energy harvesting can often be achieved without having to deviate significantly from a direct flight path and that by being aware of the wind field that there are considerable opportunities for energy savings when flying in urban environments.

VII. Conclusions

A. Conclusions

- Urban gulls demonstrated that there is extensive environmental energy available in the urban environment, as shown by the high percentage of soaring flight during their daily commutes.
- Thermalling is a good strategy in the right conditions, with tracks suggesting that thermals are so numerous in the city that it was not necessary for the birds to use every thermal or deviate significantly from the shortest path.
- The gulls thermal slightly faster than the minimum sink speed, in what may be a trade-off between maximum energy gains and stall avoidance.
- The inter-thermalling velocities of the gulls were not full explained by CoT or StF models which suggests that both energy and time could be drivers in velocity selection.
- High levels of non-flapping flight were performed on days with low thermal availability through the combined use of orographic soaring and gliding.
- The gulls flew at their best glide velocity during orographic soaring, making adjustments to fly faster in head winds and slower in updrafts.
- For gulls flight at minimum power speed in flapping flight is close to the best glide velocity in soaring. This means the gulls can switch easily between flapping and soaring as updrafts are discovered promoting maximum energy harvesting potential.
- Adjusting for headwinds in flapping flight while maintaining a speed close to the best glide velocity requires a mechanical power increase of +6% but could result in energy savings of +31%.
- CoT optimization is suitable for use in the urban environment and should be considered in the platform design of SUAVs in order to improve flight performance.

Acknowledgments

This project has received funding from the European Research Council (ERC) under the European Union's Horizon 2020 research and innovation programme (grant agreement No. 679355) and was partially supported by the EPSRC Centre for Doctoral Training in Future Autonomous and Robotic Systems (FARSCOPE) at the Bristol Robotics Laboratory.

References

[1] Cai, G., Dias, J., and Seneviratne, L., "A survey of small-scale unmanned aerial vehicles: Recent advances and future development trends," *Unmanned Systems*, Vol. 2, No. 02, 2014, pp. 175–199.

[2] Girard, A. R., Howell, A. S., and Hedrick, J. K., "Border patrol and surveillance missions using multiple unmanned air vehicles," *2004 43rd IEEE Conference on Decision and Control (CDC)(IEEE Cat. No. 04CH37601)*, Vol. 1, IEEE, 2004, pp. 620–625.

[3] Tomic, T., Schmid, K., Lutz, P., Domel, A., Kassecker, M., Mair, E., Grixa, I. L., Ruess, F., Suppa, M., and Burschka, D., "Toward a fully autonomous UAV: Research platform for indoor and outdoor urban search and rescue," *IEEE robotics & automation magazine*, Vol. 19, No. 3, 2012, pp. 46–56.

[4] Thiels, C. A., Aho, J. M., Zietlow, S. P., and Jenkins, D. H., "Use of unmanned aerial vehicles for medical product transport," *Air medical journal*, Vol. 34, No. 2, 2015, pp. 104–108.

[5] Murray, C. C., and Chu, A. G., "The flying sidekick traveling salesman problem: Optimization of drone-assisted parcel delivery," *Transportation Research Part C: Emerging Technologies*, Vol. 54, 2015, pp. 86–109.

[6] Watkins, S., Milbank, J., Loxton, B. J., and Melbourne, W. H., "Atmospheric winds and their implications for microair vehicles," *AIAA journal*, Vol. 44, No. 11, 2006, pp. 2591–2600.

[7] Watkins, S., Thompson, M., Loxton, B., and Abdulrahim, M., "On low altitude flight through the atmospheric boundary layer," *International Journal of Micro Air Vehicles*, Vol. 2, No. 2, 2010, pp. 55–68.

[8] Watkins, S., Fisher, A., Mohamed, A., Marino, M., Thompson, M., Clothier, R., and Ravi, S., "The turbulent flight environment close to the ground and its effects on fixed and flapping wings at low Reynolds number," *5th European Conference for Aeronautics and Space Sciences, Munich, Germany, 1–5 July 2014*, 2013.

[9] Bronz, M., Moschetta, J. M., Brisset, P., and Gorraz, M., "Towards a long endurance MAV," *International Journal of Micro Air Vehicles*, Vol. 1, No. 4, 2009, pp. 241–254.

[10] Gavrilovic, N., Mohamed, A., Marino, M., Watkins, S., Moschetta, J.-M., and Bénard, E., "Avian-inspired energy-harvesting from atmospheric phenomena for small UAVs," *Bioinspiration & biomimetics*, Vol. 14, No. 1, 2018.

[11] Spelt, A., Williamson, C., Shamoun-Baranes, J., Shepard, E., Rock, P., and Windsor, S., "Habitat use of urban-nesting lesser black-backed gulls during the breeding season," *Scientific reports*, Vol. 9, No. 1, 2019, pp. 1–11.

[12] Klaassen, R. H., Ens, B. J., Shamoun-Baranes, J., Exo, K.-M., and Bairlein, F., "Migration strategy of a flight generalist, the Lesser Black-backed Gull Larus fuscus," *Behavioral Ecology*, Vol. 23, No. 1, 2011, pp. 58–68.

[13] McLaren, J. D., Shamoun-Baranes, J., Camphuysen, C., and Bouten, W., "Directed flight and optimal airspeeds: homeward-bound gulls react flexibly to wind yet fly slower than predicted," *Journal of Avian Biology*, Vol. 47, No. 4, 2016, pp. 476–490.

[14] Shepard, E. L., Williamson, C., and Windsor, S. P., "Fine-scale flight strategies of gulls in urban airflows indicate risk and reward in city living," *Philosophical Transactions of the Royal Society B: Biological Sciences*, Vol. 371, No. 1704, 2016, p. 20150394.

[15] Guerra-Langan, A., Araujo-Estrada, S., and Windsor, S., "UAV control costs mirror bird behaviour when soaring close to buildings," *11th International Micro Air Vehicle Competition and Conference, Spain*, 2019.

[16] White, C., Watkins, S., Lim, E., and Massey, K., "The soaring potential of a micro air vehicle in an urban environment," *International Journal of Micro Air Vehicles*, Vol. 4, No. 1, 2012, pp. 1–14.

[17] Pennycuick, C. J., "A wind-tunnel study of gliding flight in the pigeon Columba livia," *Journal of experimental Biology*, Vol. 49, No. 3, 1968, pp. 509–526.

[18] Dial, K., Biewener, A., Tobalske, B., and Warrick, D., "Mechanical power output of bird flight," *Nature*, Vol. 390, No. 6655, 1997, p. 67.

[19] Hedrick, T. L., Tobalske, B. W., and Biewener, A. A., "How cockatiels (Nymphicus hollandicus) modulate pectoralis power output across flight speeds," *Journal of Experimental Biology*, Vol. 206, No. 8, 2003, pp. 1363–1378.

[20] Tucker, V. A., and Parrott, G. C., "Aerodynamics of gliding flight in a falcon and other birds," *Journal of Experimental Biology*, Vol. 52, No. 2, 1970, pp. 345–367.

[21] Pennycuick, C., Heine, C. E., Kirkpatrick, S. J., and FULLER, M. R., "The profile drag of a hawk's wing, measured by wake sampling in a wind tunnel," *Journal of Experimental Biology*, Vol. 165, No. 1, 1992, pp. 1–19.

[22] Lentink, D., Müller, U., Stamhuis, E., De Kat, R., Van Gestel, W., Veldhuis, L., Henningsson, P., Hedenström, A., Videler, J. J., and Van Leeuwen, J. L., "How swifts control their glide performance with morphing wings," *Nature*, Vol. 446, No. 7139, 2007, p. 1082.

[23] Rosen, M., and Hedenstrom, A., "Gliding flight in a jackdaw: a wind tunnel study," *Journal of Experimental Biology*, Vol. 204, No. 6, 2001, pp. 1153–1166.

[24] Alerstam, T., and Lindström, Å., "Optimal bird migration: the relative importance of time, energy, and safety," *Bird migration*, Springer, 1990, pp. 331–351.

[25] Åkesson, S., and Hedenström, A., "Wind selectivity of migratory flight departures in birds," *Behavioral Ecology and Sociobiology*, Vol. 47, No. 3, 2000, pp. 140–144.

[26] Alerstam, T., "Optimal bird migration revisited," *Journal of Ornithology*, Vol. 152, No. 1, 2011, pp. 5–23.

[27] Pennycuick, C. J., *Modelling the flying bird*, Vol. 5, Elsevier, 2008.

[28] MacCready, P. B., "Optimum airspeed selector," *Soaring (January–February)*, Vol. 10, No. 11, 1958.

[29] Lawrance, N. R., and Sukkarieh, S., "Autonomous exploration of a wind field with a gliding aircraft," *Journal of guidance, control, and dynamics*, Vol. 34, No. 3, 2011, pp. 719–733.

[30] Taylor, G. K., Reynolds, K. V., and Thomas, A. L., "Soaring energetics and glide performance in a moving atmosphere," *Philosophical Transactions of the Royal Society B: Biological Sciences*, Vol. 371, No. 1704, 2016.

[31] Hedrick, T. L., Pichot, C., and De Margerie, E., "Gliding for a free lunch: biomechanics of foraging flight in common swifts (Apus apus)," *Journal of Experimental Biology*, Vol. 221, No. 22, 2018, p. jeb186270.

[32] Pennycuick, C. J., "Thermal soaring compared in three dissimilar tropical bird species, Fregata magnificens, Pelecanus occidentals and Coragyps atratus," *Journal of Experimental Biology*, Vol. 102, No. 1, 1983, pp. 307–325.

[33] Pennycuick, C. J., "Field observations of thermals and thermal streets, and the theory of cross-country soaring flight," *Journal of Avian Biology*, 1998, pp. 33–43.

[34] Ákos, Z., Nagy, M., Leven, S., and Vicsek, T., "Thermal soaring flight of birds and unmanned aerial vehicles," *Bioinspiration & biomimetics*, Vol. 5, No. 4, 2010.

[35] Bouten, W., Baaij, E. W., Shamoun-Baranes, J., and Camphuysen, K. C., "A flexible GPS tracking system for studying bird behaviour at multiple scales," *Journal of Ornithology*, Vol. 154, No. 2, 2013, pp. 571–580.

[36] Shamoun-Baranes, J., Bouten, W., van Loon, E. E., Meijer, C., and Camphuysen, C., "Flap or soar? How a flight generalist responds to its aerial environment," *Philosophical Transactions of the Royal Society B: Biological Sciences*, Vol. 371, No. 1704, 2016.

[37] EnvironmentalAgency, "LIDAR Composite DEM," , October 2019. URL `https://data.gov.uk/dataset/lidar-composite-dtm-2m`.

[38] MetOffice, "Unified Model," , November 2017. URL `https://www.metoffice.gov.uk/research/modelling-systems/unified-model`.

[39] Data SIO, U. N. N. G., NOAA, "51°29'52.84"N,2°33'20.72W"," , October 2019, GOOGLE EARTH, Getmapping, 4.19.2018.

[40] Langelaan, J., "Biologically inspired flight techniques for small and micro unmanned aerial vehicles," *AIAA guidance, navigation and control conference and exhibit*, 2008, p. 6511.

[41] Bonnin, V., Bénard, E., Moschetta, J.-M., and Toomer, C., "Energy-harvesting mechanisms for UAV flight by dynamic soaring," *International Journal of Micro Air Vehicles*, Vol. 7, No. 3, 2015, pp. 213–229.

[42] Gudmundsson, S., Golubev, V. V., Drakunov, S., and Reinholtz, C., "Bio-Inspired Opportunistic Approaches in Energy-Conserving/Harnessing Flight-Path Modeling for UAS," *AIAA Modeling and Simulation Technologies Conference*, 2016, p. 3676.

[43] Liu, D.-N., Hou, Z.-X., Guo, Z., Yang, X.-X., and Gao, X.-Z., "Bio-inspired energy-harvesting mechanisms and patterns of dynamic soaring," *Bioinspiration & biomimetics*, Vol. 12, No. 1, 2017, p. 016014.

[44] Taha, H., "Urban climates and heat islands: albedo, evapotranspiration, and anthropogenic heat," *Energy and buildings*, Vol. 25, No. 2, 1997, pp. 99–103.

[45] Stone Jr, B., and Rodgers, M. O., "Urban form and thermal efficiency: how the design of cities influences the urban heat island effect," *American Planning Association. Journal of the American Planning Association*, Vol. 67, No. 2, 2001, p. 186.

[46] Eshelby, M., *Aircraft performance: Theory and practice*, American Institute of Aeronautics and Astronautics, Inc., 2000.

[47] Welch, A., Irving, F., and Welch, L., *New soaring pilot*, Murray, 1977.

[48] Pennycuick, C., "The soaring flight of vultures," *Scientific American*, Vol. 229, No. 6, 1973, pp. 102–109.

[49] Piggott, D., *Understanding gliding: the principles of soaring flight*, Barnes & Noble, 1977.

[50] Makovkin, D., and Langelaan, J. W., "Optimal persistent surveillance using coordinated soaring," *AIAA Guidance, Navigation, and Control Conference*, 2014, p. 0261.

[51] Regulations, F. A., "Part 23 Airworthiness Standards: Normal, Utility, Acrobatic and Commuter Category Airplanes," , 1991.

[52] Mohamed, A., Abdulrahim, M., Watkins, S., and Clothier, R., "Development and flight testing of a turbulence mitigation system for micro air vehicles," *Journal of Field Robotics*, Vol. 33, No. 5, 2016, pp. 639–660.

[53] Araujo-Estrada, S. A., Salama, F., Greatwood, C. M., Wood, K. T., Richardson, T. S., and Windsor, S. P., "Bio-inspired distributed strain and airflow sensing for small unmanned air vehicle flight control," *AIAA Guidance, Navigation, and Control Conference*, 2017, p. 1487.

[54] Callou, F., and Foinet, G., "Method for controlling a multi-rotor rotary-wing drone, with cross wind and accelerometer bias estimation and compensation," , Nov. 8 2016. US Patent 9,488,978.

[55] Mohammed, F., Idries, A., Mohamed, N., Al-Jaroodi, J., and Jawhar, I., "UAVs for smart cities: Opportunities and challenges," *2014 International Conference on Unmanned Aircraft Systems (ICUAS)*, IEEE, 2014, pp. 267–273.

[56] Menouar, H., Guvenc, I., Akkaya, K., Uluagac, A. S., Kadri, A., and Tuncer, A., "UAV-enabled intelligent transportation systems for the smart city: Applications and challenges," *IEEE Communications Magazine*, Vol. 55, No. 3, 2017, pp. 22–28.

VIII. Appendix

A. Ground speeds

The soaring strategy velocity responses for wind direction were also generated in the ground speed frame in order to demonstrate that the results were not caused by false correlation from using the wind data set in the measured and modelled data. The ground speed models shown in figure 10 agree with the airspeed results from section V.C, showing a trend of flying faster in high-altitude inter-thermal flight and slower in strategies which take advantage of updrafts.

All plots show resulting ground speed from the optimized airspeed using CoT modelling with the horizontal wind, the central line indicates has no vertical wind. Upper and lower lines shows a down draft and up draft respectively both of 0.5ms^{-1} strength. A Gaussian smoothing filter of 5σ was applied to the GPS fixes to demonstrate density.

Additionally, the Pearson R correlation coefficients were calculated for the measured velocity responses compared to model data generated using a) measured wind data and b) a randomized sample from the same wind data population. The tests were performed for flapping flight, and orographic and low-altitude gliding flight combined. In both cases there was no correlation between the model and the measured data when the model was generated using a random sample, and a relatively high correlation between the model and measured data when the model was generated using measured wind data. Results as follows: flapping flight ($R = 0.6, RMSE = 3.12, n > 10000, p < 0.001$) flapping flight randomized sample ($R = 0.004, RMSE = 4.88, n > 10000, p < 0.001$) orographic and low-altitude flight combined ($R = 0.65, RMSE = 3.41$), orographic and low-altitude flight randomized sample ($R = -0.01, RMSE = 5.39, n > 10000, p < 0.001$).

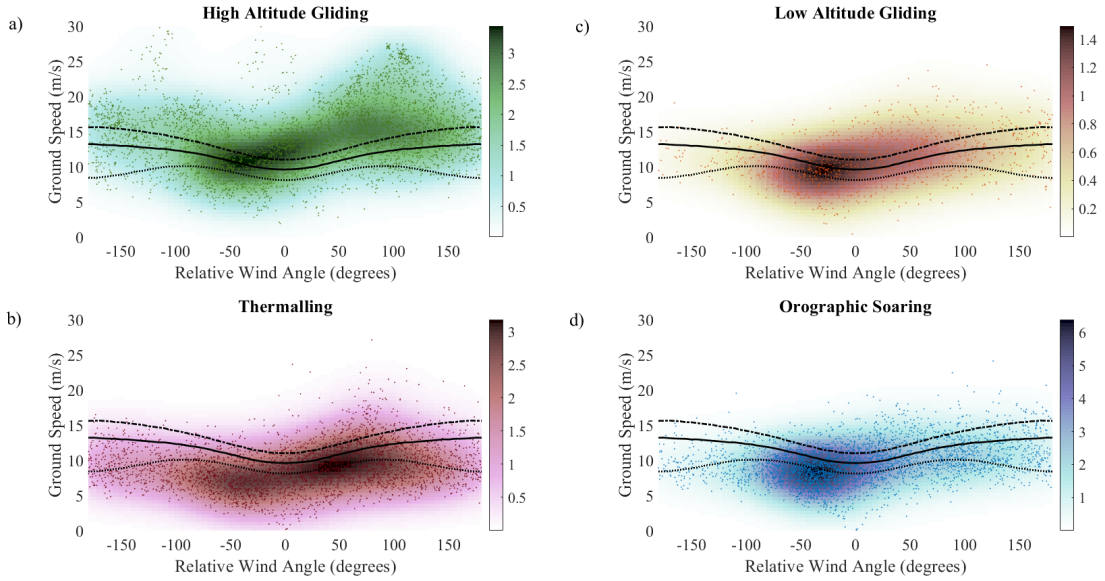

Fig. 10 Ground speed variation with the relative wind angle compared to CoT for strategies a) High altitude gliding b) Thermal soaring c) Low altitude gliding d) Orographic soaring

B. Flight Envelope

The flight envelope of a lesser black-backed gull was calculated using the size characteristics of the average lesser black-backed gull and the FAR regulations regarding wing loading [51], shown in Figure 11 a. A flight envelope charts the velocity versus the load factor and shows the performance safety limits of an aircraft. The important velocities in the flight envelope are the stall speed, U_{stall}, manoeuvre speed, U_a, cruise speed, U_c, never exceed or maximum operating speed, U_ne, and finally, the maximum dive speed, U_d. Normal flight operation occurs between U_a and U_c. The velocities from the performance curves were also added. These are labelled as, minimum sink velocity, U_{ms}, best glide velocity, U_{bg}, minimum power velocity, U_{mp}, and maximum range velocity, U_{mr}. Interestingly, the performance velocities are all in the slower region of the flight envelope and contain the majority of the recorded airspeed, as shown in the histogram in Figure 11 b.

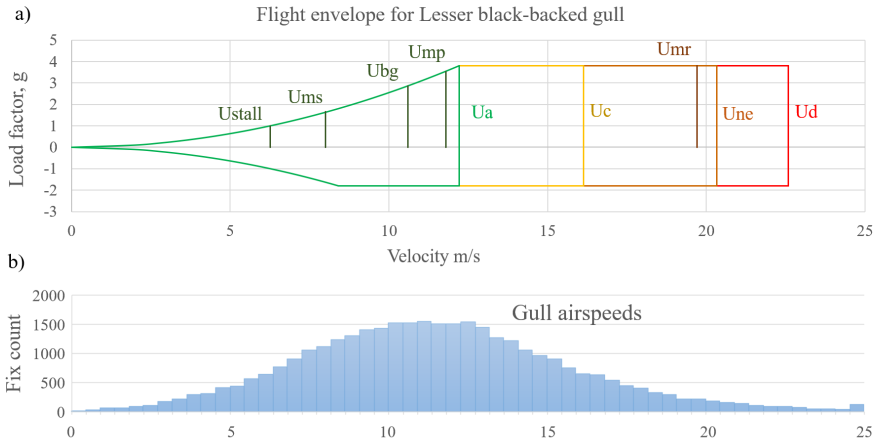

Fig. 11 a) Flight envelope for the average lesser black-backed gull using FAR regulations [51]. b) Histogram of airspeeds recorded in this study.